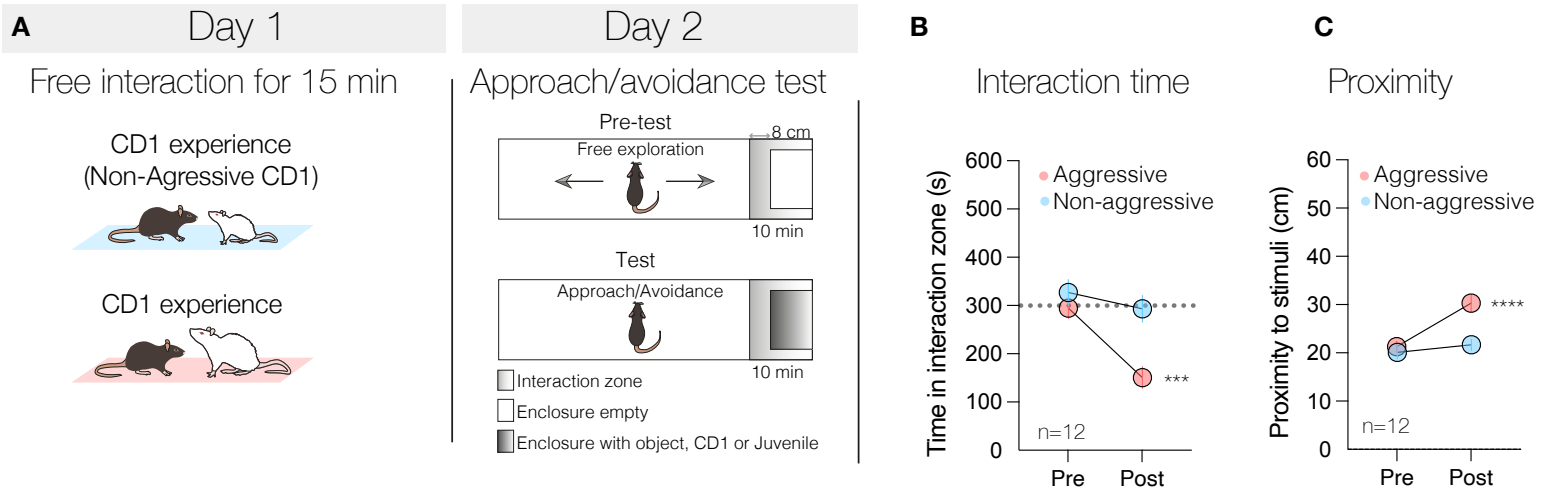

Fig S1. Aggression induces avoidance learned behavior. (A) Mice were exposed to aggressive and non-aggressive CD1s for 15 minutes. Twenty-four hours later, the animals were placed in a new arena, and after 10 minutes of free exploration with an empty enclosure, an enclosure containing the previous day's stimuli was introduced. (B) Time spent in the interaction zone on day 2. (C) Proximity to the stimulus mouse on day 2.

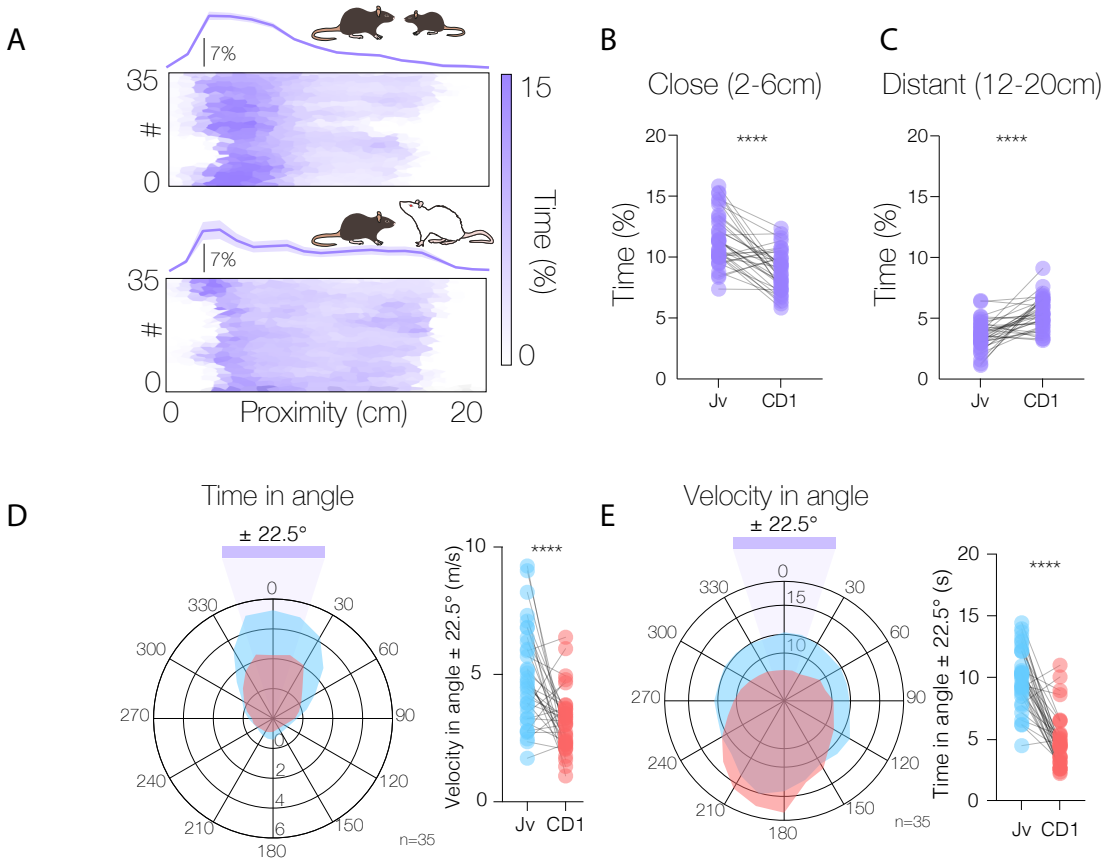

Fig S2. Quantitative analysis of free social interaction tracked with DeeplabCut. (A) Heat-maps of spatial proximity (0–20 cm) between the experimental mouse and the stimulus mouse, displayed in 5-s bins. Darker colour indicate longer occupancy. The line above each heat-map shows the mean occupancy across all distances for that animal; each horizontal lane represents one animal (n = 35). (B) Time each mouse spent in close proximity (2–6 cm) under the juvenile- and CD1-stimulus conditions. (C) Time each mouse spent in distant proximity (12–20 cm) under the same two conditions. **** P < 0.0001, paired two-tailed t-test (B,C). (D) Polar plot of angular occupancy: the experimental mouse is centred at 0°, and the location of the stimulus mouse is plotted relative to the experimental mouse's head direction. With a juvenile stimulus, focal mice spent more time in the ±22.5° sector (purple wedge) than with a CD1 stimulus, indicating increased face-to-face orientation. Right: sector occupancy quantified for both conditions. **** P < 0.0001, paired two-tailed t-test. (E) Polar plot of stimulus-mouse velocity vectors relative to the experimental mouse. Juvenile stimuli show greater occupancy in the rear sector (157.5–202.5°), consistent with the escape behaviour observed during CD1 interactions, whereas occupancy in the frontal sector is higher for juveniles, indicating more approach bouts. Right: sector occupancy quantified for both conditions.**** P < 0.0001, paired two-tailed t-test. Data are shown for all animals (n = 35).

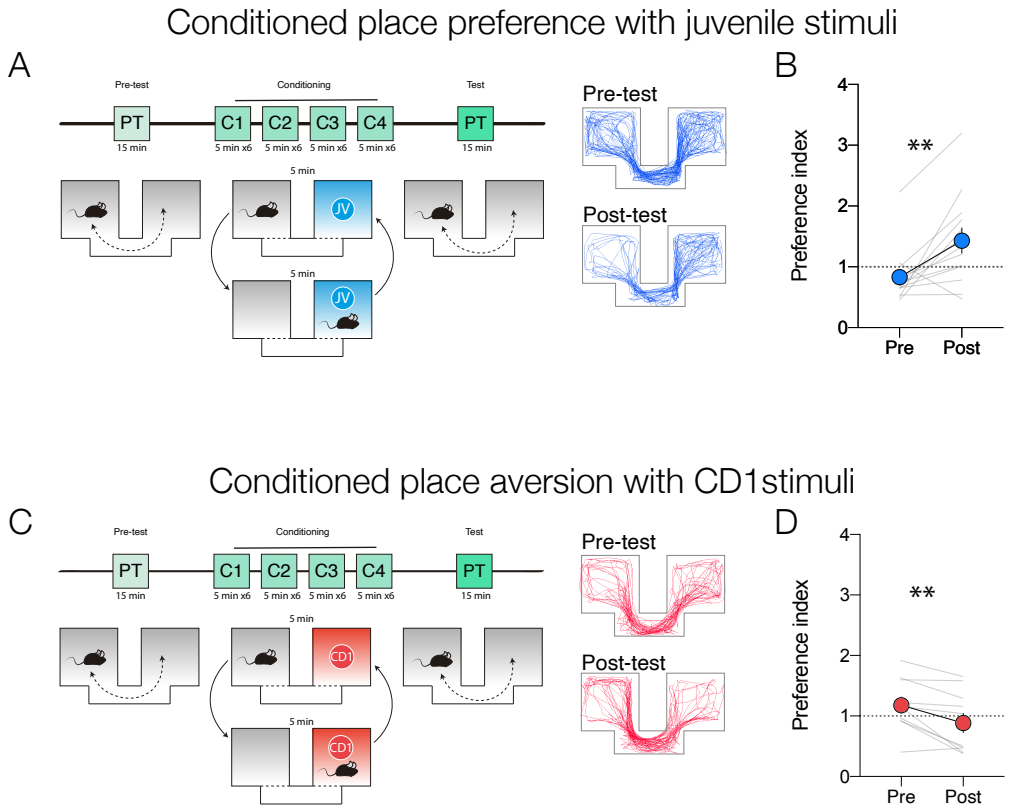

Fig S3. Rewarding versus aversive social stimuli drive conditioned place preference (CPP) and conditioned place aversion (CPA). (A) CPP paradigm (schematic). Day 0 (pre-test): Each experimental mouse freely explored both chambers for 15 min to establish its baseline preference, while its social stimulus mouse was habituated for 15 min in the chamber it would later occupy (PT). Days 1 – 4 (conditioning: C1-C4): Six alternating 5-min epochs were run each day (total 30 min). During "social" epochs the experimental mouse was confined with the stimulus mouse; during "non-social" epochs it was confined to the opposite, empty chamber. The animal was gently guided through the connecting corridor between epochs. The identity of the first epoch ("social" vs. "non-social") was counter-balanced across animals and days. (B) CPP outcome. Left, representative traces of positional tracking on the final conditioning day. Right, quantification of place preference. The preference index (PI) was calculated as time in empty chamber divided by the time in social chamber. PI < 1 indicates a preference for the social chamber. Bars show mean ± SEM; ** $p < 0.001$, paired two-tailed Student's t-test. (C) CPA paradigm (schematic). Identical to (A) except that the social stimulus was an unfamiliar adult CD-1 mouse, which is typically perceived as aggressive/aversive by the experimental C57BL/6J mouse. (D) CPA outcome. Left, representative traces on the final conditioning day. Right, PI calculated as in (B); PI > 1 indicates avoidance of the social chamber. Bars show mean ± SEM; ** $p < 0.001$, paired two-tailed Student's t-test.

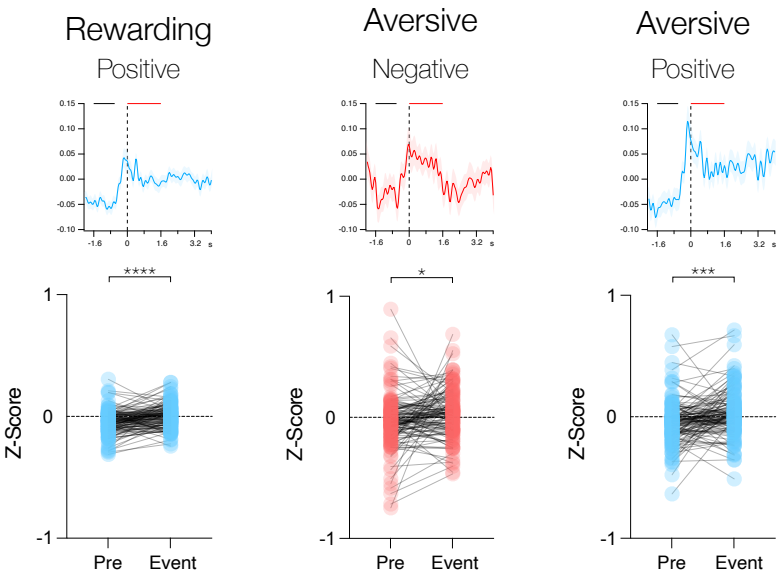

Figure S4. D1+ LNAc Neurons Respond to Both Positive and Negative Contacts. The figure shows the perievent time histograms (PETHs) for positive and negative contacts during rewarding and aversive experiences for LNAc D1+ neurons. The black line on top of the signal represents the pre-event average window (-1.6s to -0.6s before the event), and the red line represents the perievent average window (0s to 1.6s). The average windows (pre-event and perievent) were calculated for each cell and compared using a paired t-test. * $p = 0.0122$, *** $p = 0.0002$, **** $p < 0.0001$.

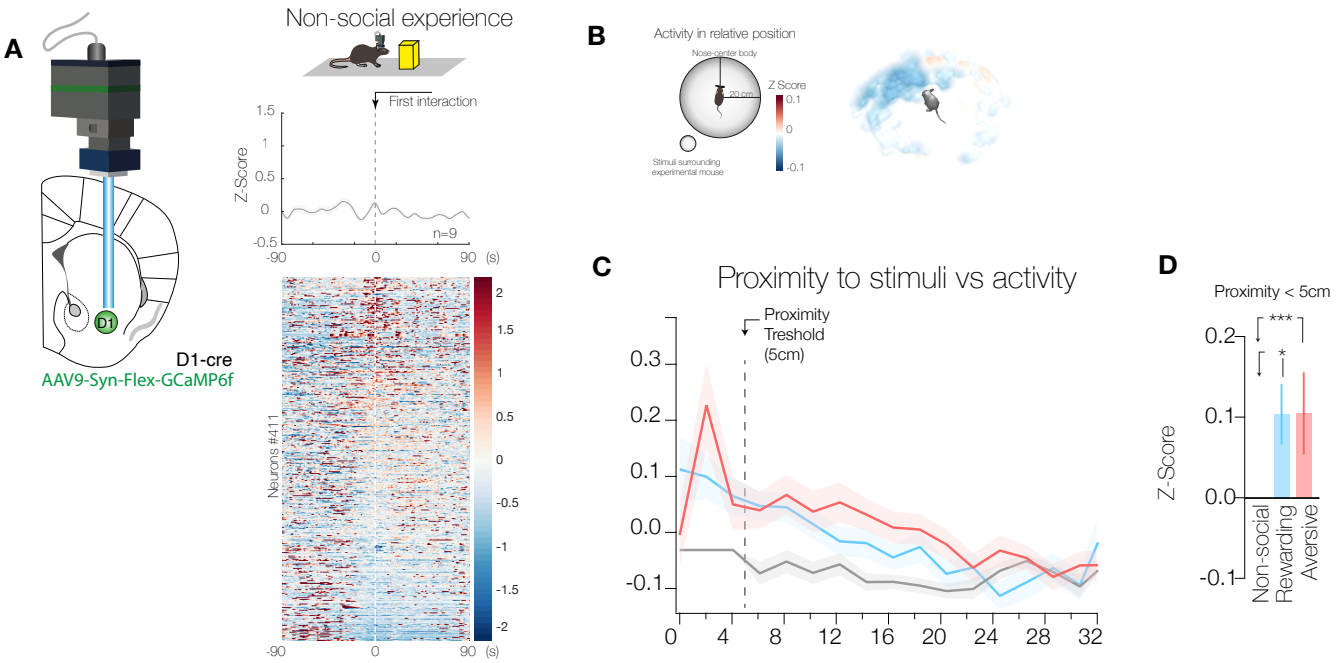

Fig S5. D1+-NAc neurons do not respond to objects but to proximity. (A) Schematic of injection and implantation sites. To the right, average activity during a rewarding experience aligned with the first interaction. The heatmap represents the activity of individual neurons (each row one neuron). (B) Schematic of a 3D heatmap representing calcium activity relative to the stimuli. To the right, heatmap showing activity relative to juvenile stimuli. (C) Plot showing activity versus proximity. The dotted line represents the proximity threshold. (D) Proximity less than 5cm plotted for the three conditions.

Espinosa et al. 2025 Fig supp 5

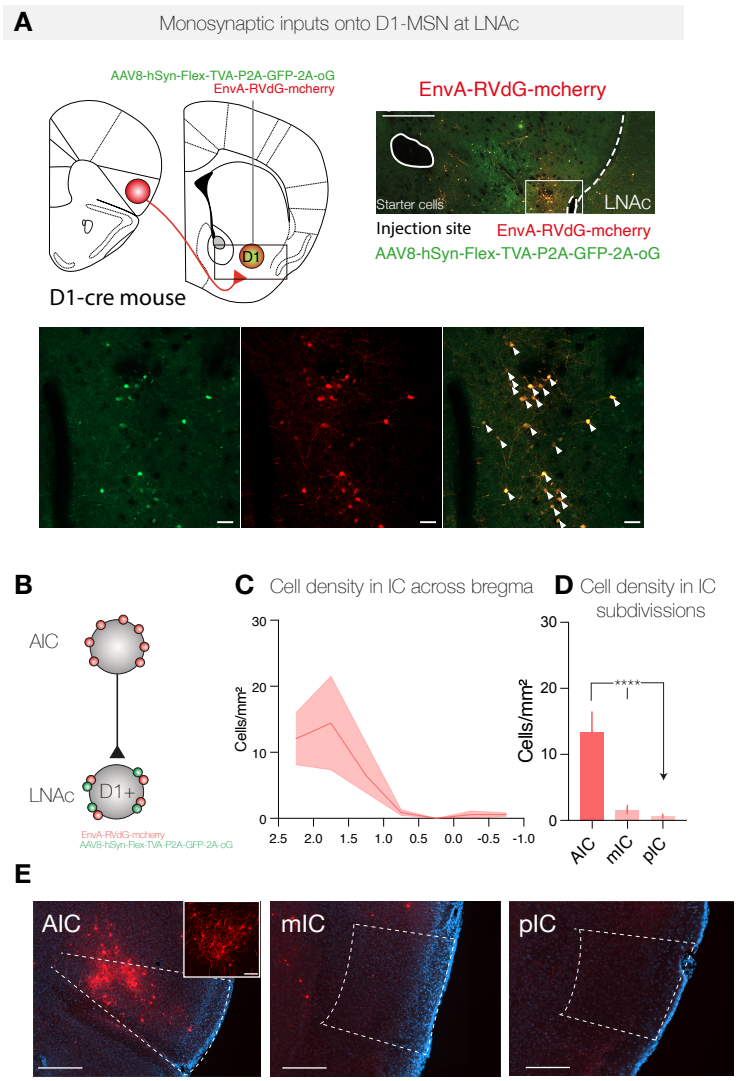

Fig S6. Anatomical characterization of AIC monosynaptic inputs onto D1-MSN of LNAc. (A) Schematic showing viral injection (scale: 500 µm) and the right panel displaying a representative picture of the injection site. Below, a magnified view of the injection site (scale: 50 µm). (B) Schematic illustrating the mechanism of rabies viral expression. (C) Cell density across the rostro-caudal axis of mCherry positive neurons. (D) Same quantification across different insular subdivisions. One-way ANOVA was used as the statistical test, with ****p<0.0001 being significant. (E) Representative pictures in each insular subdivision (scale: 500 µm), with a magnified confocal image in AIC (scale: 100 µm), n=3.

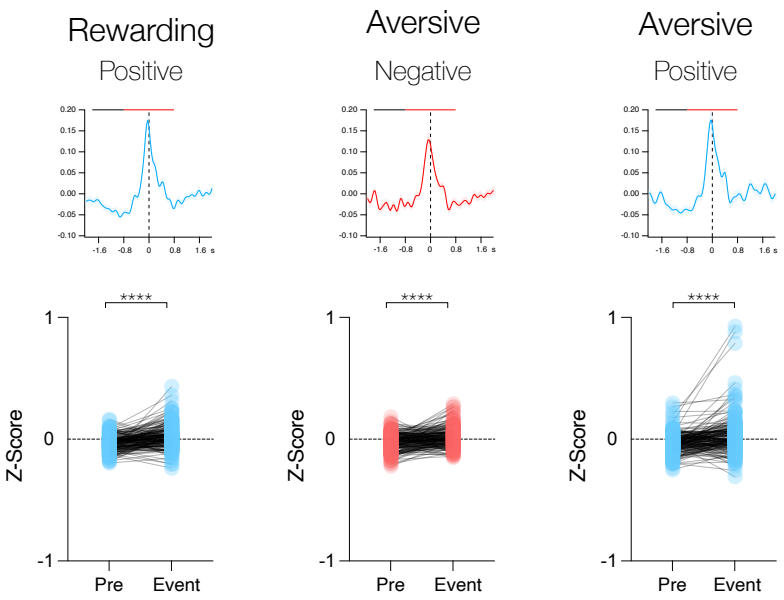

Fig S7. D1+ AIC Neurons Respond to Both Positive and Negative Contacts The figure shows the perievent time histograms (PETHs) for positive and negative contacts in rewarding and aversive experiences for AIC D1+ neurons. The black line on top of the signal represents the pre-event average windows (-1.8s to -0.8s before event) and the red line represent the perievent average windows (from -0.8s to 0.8s). The averages windows (pre.event and perievent) were calculated for each cells and compared using a paired t-test. **** <0.0001.

Espinosa et al. 2025 Fig supp 7

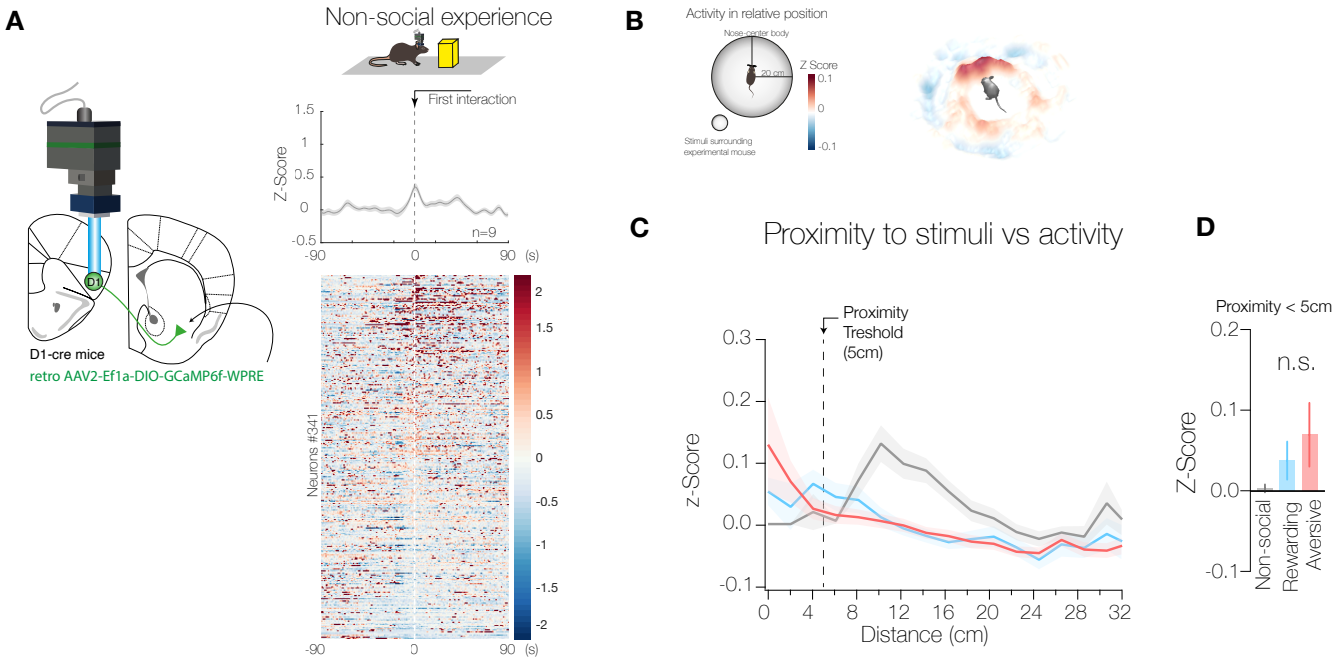

Fig S8. D1+-AIC neurons do not respond to object or proximity. (A) Schematic of injection and implantation sites. To the right, average activity during a rewarding experience aligned with the first interaction. The heatmap represents the activity of individual neurons (each row one neuron). (B) Schematic of a 3D heatmap representing calcium activity relative to the stimuli. To the right, heatmap showing activity relative to juvenile stimuli. (C) Plot showing activity versus proximity. The dotted line represents the proximity threshold. (D) Proximity less than 5cm plotted for the three conditions.

Espinosa et al. 2025 Fig supp 8

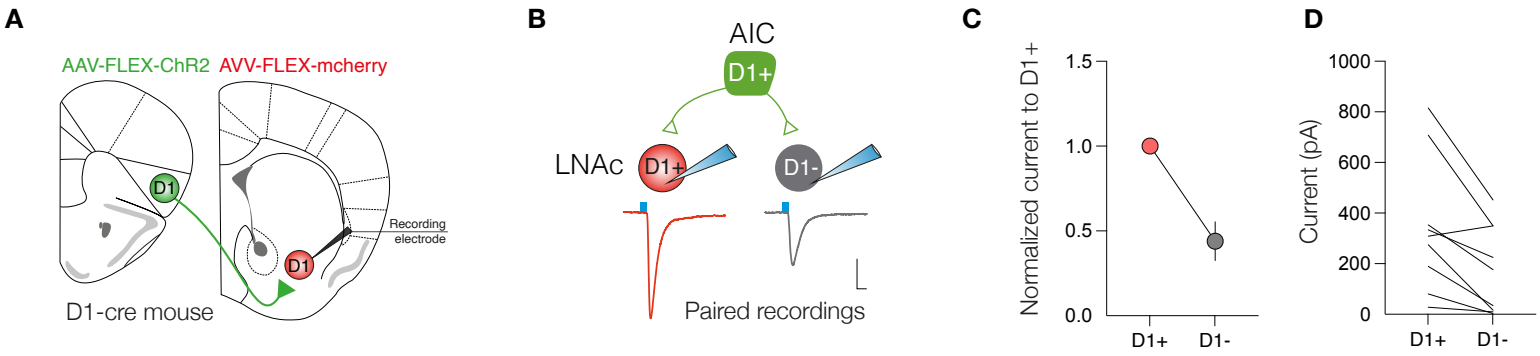

Fig S9. Preferential D1+-D1+ synaptic connection. (A) Schematic representation of viral injections into the lateral nucleus accumbens (LNAc) and the anterior insular cortex (AIC). (B) Diagram and representative trace of paired whole-cell recordings from $D1^+$ and $D1^-$ medium spiny neurons (MSNs) in the LNAc, showing responses to optogenetic stimulation of AIC afferents. (C) Left: Normalized synaptic current amplitude across recorded pairs. Right: Net current comparison for each $D1^+$ –$D1^-$ cell pair, highlighting preferential input onto $D1^+$ MSNs.

Espinosa et al. 2025 Fig supp 9

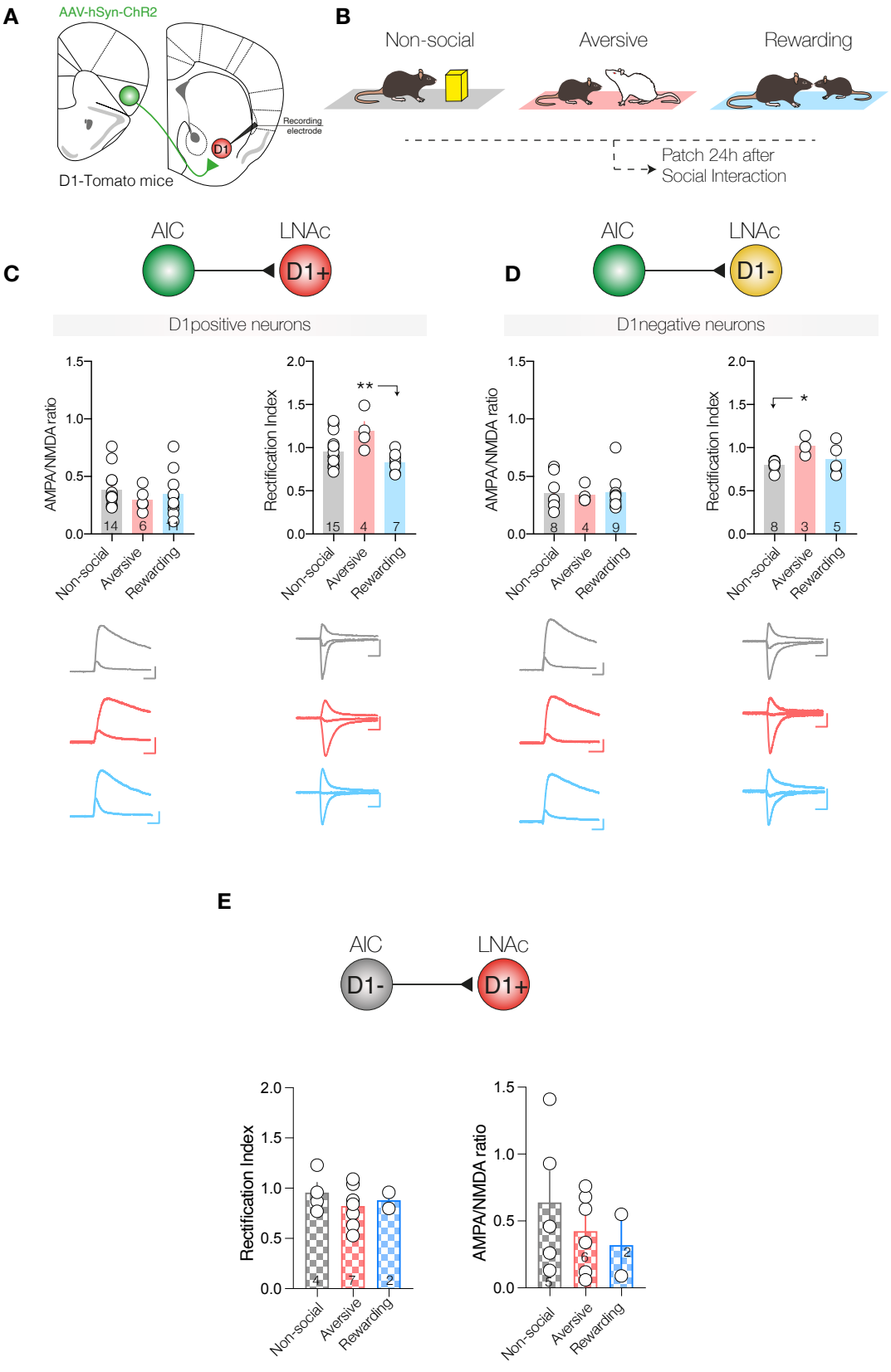

Espinosa et al. 2025 Fig supp 10

Fig S10. hSyn promoter channelrhodopisn expression in AIC neurons does not elicit synaptic plasticity after social interaction. (A) Scheme of viral injection and patch recordings. (B) Protocol of free social interaction as previously described. Same as Fig 5. (C) AMPA/NMDA ratio, with non-social versus juvenile p>0.9999, non-social versus aversive p=0.7779. To the right, the rectification index in D1-MSN, with non-social vs juvenile p=0.3941, non-social versus aversive p=0.0747, and **p=0.0095, indicating a lack of plasticity after social interaction. (D) AMPA/NMDA ratio (p>0.9999 for all conditions) and rectification index in D1 negative-MSN, with non-social versus juvenile p>0.9999 and *=p=0.0405, also indicating a lack of plasticity after social interaction. Below are the representative traces for each group. Scale: 10ms/100pA. One-way ANOVA was used as the statistical test. (E) Cre-negative control: (E) Control experiment, expression of ChR2 in D1-Cre negative neurons: AAV-hSyn-DO-ChR2-eYFP was injected into the AIC and AAV-FLEX-mCherry into the LNAc to visualise $D1^{+}$ neurons. Behavioural protocol and recordings matched previously described (B–D). Neither AMPA/NMDA ratio nor RI differed across conditions (one-way ANOVA, P > 0.5). Data are mean ± s.e.m.; dots represent individual cells. Statistical tests: one-way ANOVA followed by post-hoc comparisons; n.s., not significant.

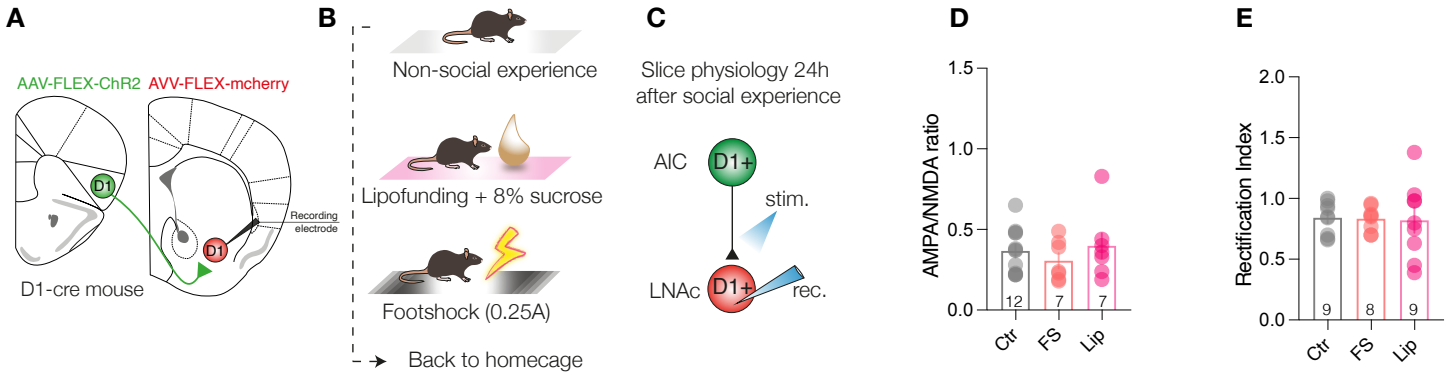

Fig S11. D1$^+$ AIC → D1$^+$ LNAc synapses encode specifically social but not general valence. (A) Viral strategy. AAV-hSyn-DIO-ChR2-eYFP was injected into the anterior insular cortex (AIC) of Drd1-Cre mice; and AAV-FLEX-mCherry into the LNAc. (B) Non-social valence test: Mice were exposed for 15 min to one of three conditions: Neutral – empty cage (home-cage context). Appetitive – 1mL (max quantity, see methods) Lipofundin + 8 % sucrose (palatable reward). Aversive – eight random foot-shocks (0.25 mA, 500 ms). (C) Ex-vivo whole-cell voltage-clamp recordings in LNAc were obtained 24 h later; blue light (473 nm) selectively activated AIC terminals. (D) AMPA/NMDA current ratio did not differ across neutral, appetitive or aversive groups (one-way ANOVA, $P > 0.05$). (E) Rectification index (RI) was likewise unchanged (one-way ANOVA, $P > 0.05$). Bars represent mean ± s.e.m.; dots, individual cells. These results indicate that plasticity at AIC → lNAc D1-synapses is selectively driven by social valence and is insensitive to non-social positive or negative experiences.

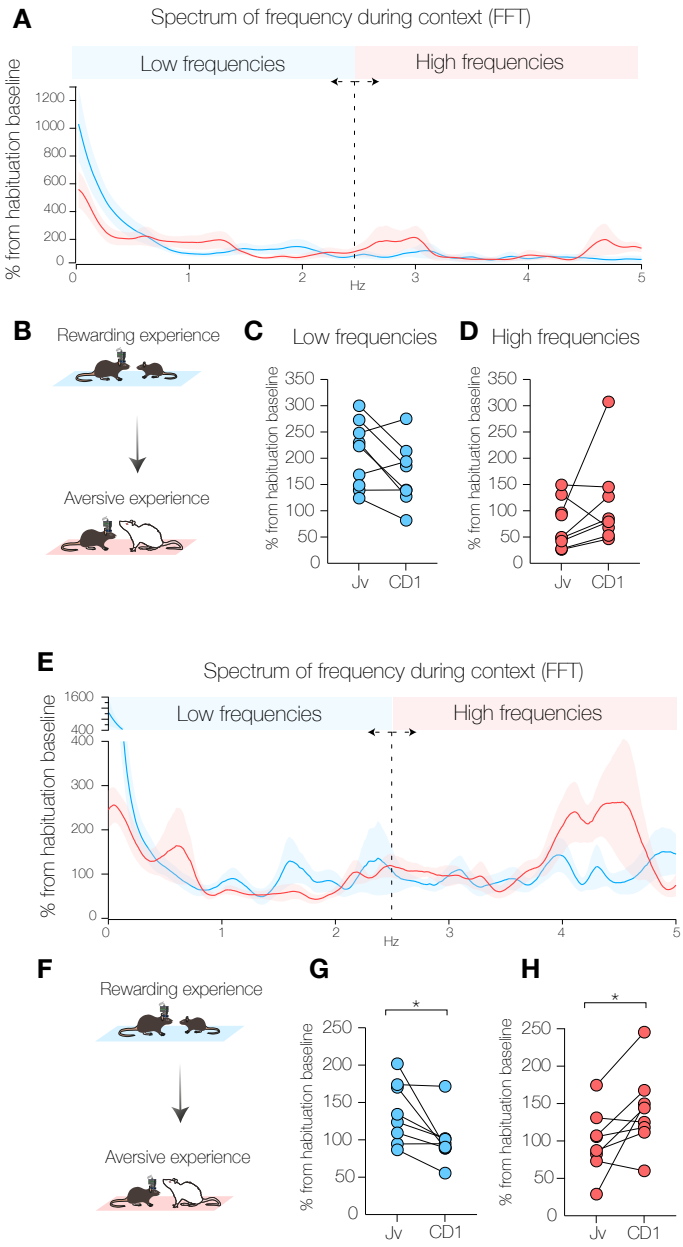

Fig S12. Frequency-domain analysis of calcium transients in LNAc and AIC neurons. Lateral nucleus accumbens (LNAc): (A) Mean power-spectral density (PSD) of ΔF/F calcium traces obtained via Fast-Fourier Transform (FFT) during first exposure to juvenile and subsequent exposure to CD1. Shaded areas indicate ± s.e.m. (B) Behavioural timeline: mice sequentially encountered juvenile (rewarding) and CD1 (aversive) stimuli in the same context, separated by 24 h. (C) Quantification of low-frequency band (0–2.5 Hz) power per neuron comparing juvenile and CD1 conditions. (D) Quantification of high-frequency band (2.5–5 Hz) power per neuron across both exposures. (n = 9 mice). Anterior insular cortex (AIC): (E–H) Analogous analyses performed on AIC neurons using the same behavioural protocol: PSD spectra (E), behavioural timeline (F), low-frequency power (G), and high-frequency power (H). All comparisons in LNAc or AIC involved the same neurons recorded across both behavioural sessions. Data points represent individual mice (n = 8 mice). Statistics: paired two-tailed t-test; n.s., not significant (P > 0.05).

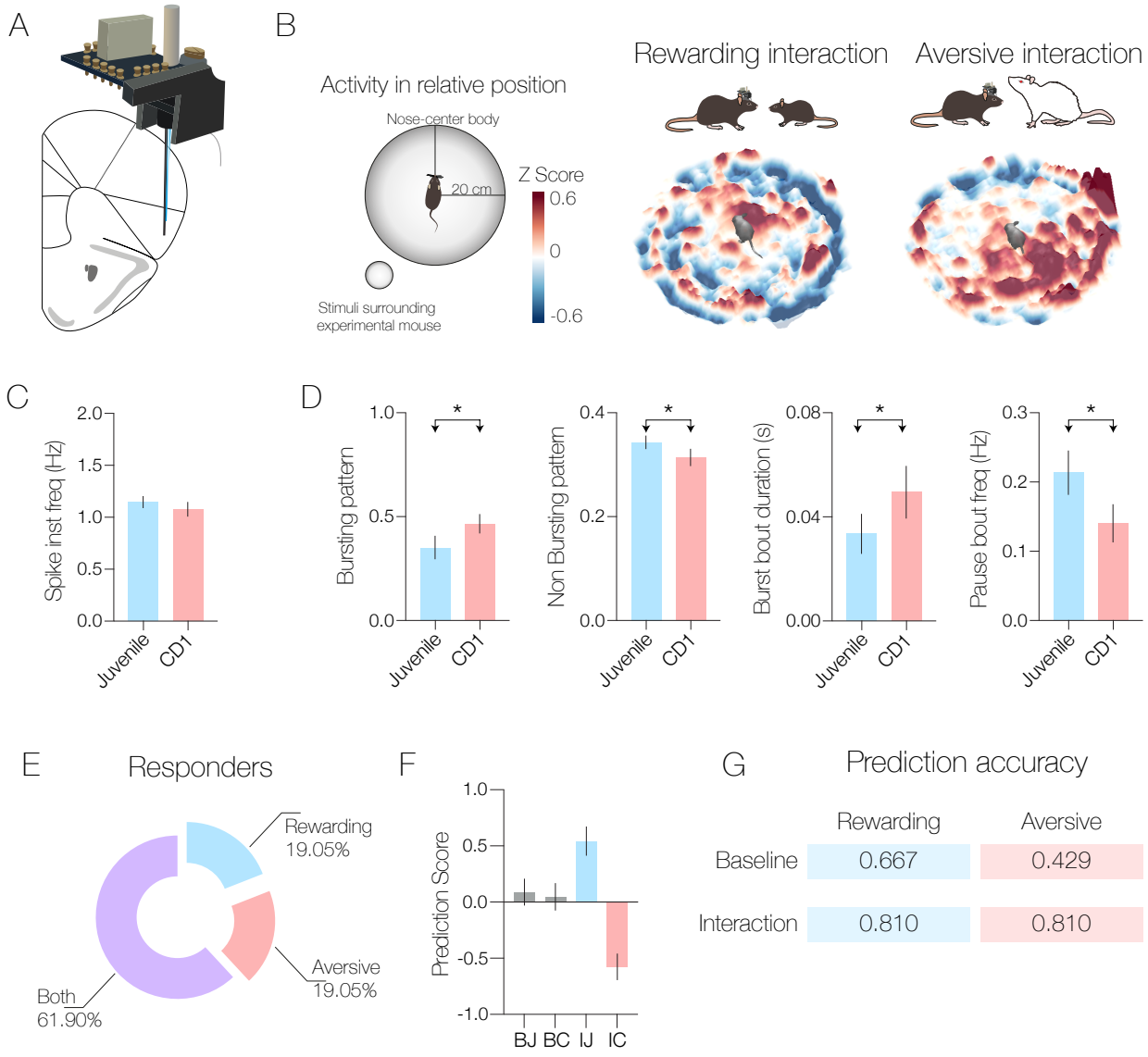

Fig. S13 In-vivo spiking dynamics of AIC neurons during rewarding and aversive social encounters. (A) Schematic of eight-tetrode bundle implanted in the AIC. (B) Schematic of a 3D heatmap representing spike activity (z-scored) relative to the stimuli (juvenile and CD1). Warmer colours denote higher firing probability. (C) Average instantaneous firing rate (mean ± s.e.m.) is similar for the two situations (paired two-tailed t-test, n.s.). (D) Burst analysis. Compared with juvenile sessions, CD-1 exposure produced: a higher fraction of spikes occurring in bursts, fewer isolated spikes, longer bursts, and shorter pauses between bursts ($P < 0.05$, paired two-tailed t-tests). (E) Response selectivity of single units: 62 % responded to both stimuli, 19 % only to the juvenile, and 19 % only to the CD-1. (F) A support-vector-machine (SVM) classifier trained on basic firing-pattern features distinguished juvenile from CD-1 encounters with high accuracy. (G) Confusion matrix from 5-fold cross-validation illustrating the classifier's performance. Data come from 42 well-isolated neurons recorded in 12 mice; bars show mean ± s.e.m., dots represent individual units.

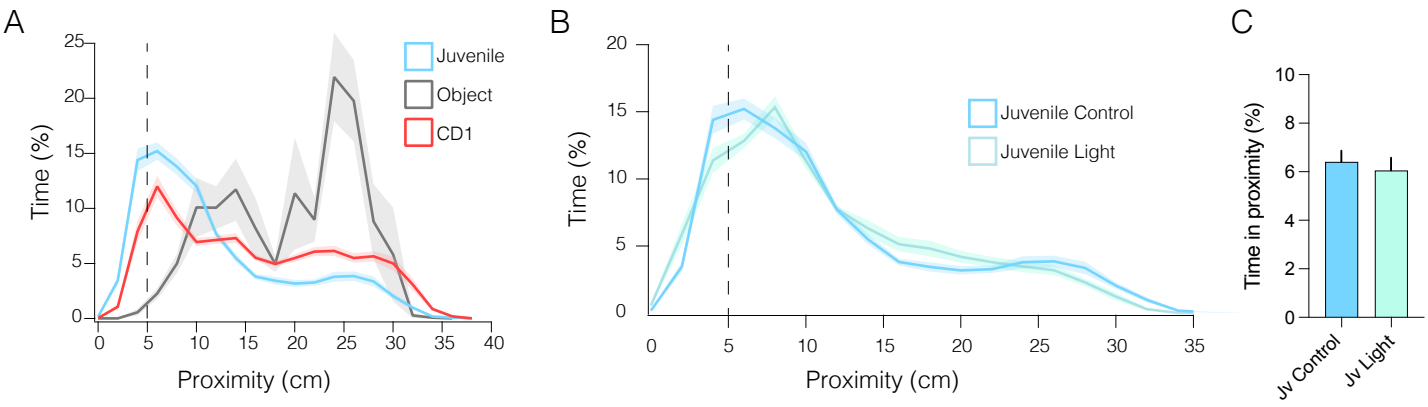

Fig. S14 Proximity behaviour is unaffected by light delivery alone. (A) Time spent by the experimental mouse in proximity to a juvenile conspecific, an aggressive adult CD-1 mouse, or an inanimate object. (B) Comparison of the juvenile condition between control sessions (no illumination; data reproduced from A) and sessions with blue-light stimulation delivered to the nucleus accumbens during interaction bouts (same optogenetic protocol as in Fig. 7). (C) Light delivery alone did not alter proximity behaviour (unpaired two-tailed t-test, n.s., control: n = 35 mice, light: n= 8 mice). These results confirm that the stimulation parameters used in the main experiment do not acutely influence social approach behaviour by themselves.

Espinosa et al. 2025 Fig supp 14

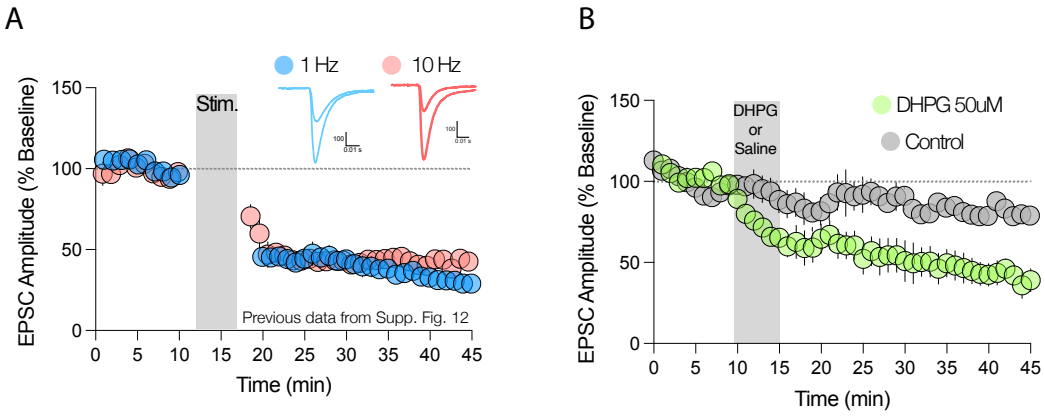

Fig. S15 Group I mGluR activation also induces LTD at AIC → LNAc synapses. (A) Long-term depression (LTD) evoked by optogenetic stimulation (1 Hz and 10 Hz; data reproduced from Fig. 6). (B) LTD produced by bath application of the group I mGluR agonist DHPG (50 μM) n=6 cells. "Control" traces represent time-matched recordings with neither stimulation nor drug application, n=4 cells. Together, these results show that activating mGluR1/5 reliably depresses synaptic strength in the AIC-to-LNAc pathway as optogenetic stimulation.

Espinosa et al. 2025 Fig supp 15